FLOW STRUCTURES DUE TO STATIC AND OSCILLATING DIMPLES IN CHANNEL FLOWS

Ming-Wei Ge, Chun-Xiao Xu*, Gui-Xiang Cui, Zhao-Shun Zhang

Department of Engineering Mechanics, School of Aerospace
Tsinghua University, Beijing 100084, P. R. China
*xucx@tsinghua.edu.cn

ABSTRACT

Flow structures due to static and oscillating dimple in a channel are studied by direct numerical simulation. Coordinate transform are employed to account for the time-dependent complex wall deformation. The governing equations are solved in the computational space by Fourier-Chebyshev spectral method and third-order time splitting method. Three Reynolds numbers, i.e. Re=500, 1000, 1900, and two oscillating frequencies of f=0.5 and 2 are considered. With the increase of the Re, vortical structures can be generated by the static dimple. At Re=500, periodic shedding of vortices can be observed at both frequency. At Re=1900, no significant interaction between moving dimple and outside turbulence can be found at f=0.5. By increasing the frequency of dimple oscillation to f=2, the influence of the moving dimple on outside turbulent flow can be observed.

INTRODUCTION

Flow over dimpled surfaces has drawn more and more attentions in both heat transfer and flow control research field in recent years. Dimples have the advantages of substantial heat transfer augmentation with low drag penalty (Shchukin, 1998). They can act within a continuous surface, generate more localised vorticity than pimples and are considered as an excellent candidate for flow control application (McKeon, 2004).

Flow structures due to static spherical dimple depressions on a channel surface have been studied by Ligrani (2001) and Won (2005) by experimental flow visualization. In Ligrani (2001), the ratio of maximum dimple depth to dimple print diameter is fixed to 0.2, and three different channel heights are used so that the ratio of channel heights to dimple print diameter takes the value of 0.25, 0.5 and 1.0, respectively. For all the three ratios, a primary vortex pair shedding from the central portion of each dimple was observed, and the nondimensional shedding frequencies of 2.2-3.0 were reported. In Won (2005), the influence of dimple depths on flow structures are investigated. The ratio of channel heights to dimple print diameter are fixed to 1, and the ratio of the maximum dimple depths to dimple print diameter takes three values of 0.1, 0.2 and 0.3. Periodic vortex pair ejections from the central part of the dimple were observed for all the three different dimples. Bigger and stronger vortices are produced by deeper dimples. McKeon (2004) studied the vorticity generation by active dimples by numerical simulation and experimental visulization. In their simulation the influence of the dimples was simplified by imposing perturbation velocity conditions at the bottom wall, and the flow separation within the dimples can not been represented. Hence further investigations into the flow over dimpled surface are needed to get more quantitative knowledge about the influence of the dimple on the flow above, especially for active dimples.

In present study, the flows in a plane channel with a static or oscillating dimple on the lower wall are studied by direct numerical simulation. If the maximum depth and print diameter of the dimple are represented respectively by H and D, the dimple oscillating frequency is f, then the flow in the channel depends on H, D, f, δ, U and ν, in which δ is the channel half width, U the bulk mean velocity and ν the kinetic viscosity of the fluid (for incompressible fluid, the density ρ is considered as a known constant). According to dimensional analysis, the flow is determined by the following four dimensionless parameters: the ratio of dimple print diameter to channel half width $D^* = D / \delta$, the ratio of dimple depth to diameter $\varepsilon = H / D$, Reynolds number $Re = U\delta / \nu$ and Strouhal number $St = fD / U$. In present study, the dimples with fixed D^* and ε are employed, and the main concern is focused on the influence of Re and St on the flow structures.

NUMERICAL METHOD

The flow of incompressible Newtonian fluid in a channel with dimpled walls is governed by Navier-Stokes equation and continuity equation:

$$\frac{\partial u_i}{\partial t} + u_j \frac{\partial u_i}{\partial x_j} = -\frac{1}{\rho} \frac{\partial p}{\partial x_i} + \nu \frac{\partial^2 u_i}{\partial x_j \partial x_j} \qquad (1)$$

$$\frac{\partial u_i}{\partial x_i} = 0 \qquad (2)$$

In streamwise (x or x_1) and spanwise (z or x_3) directions, the flow is assumed periodic. In wall normal direction (y or x_2), the no-slip condition is used at the walls.

Let the upper and lower walls are located at $y = 1 + \eta_u$ and $y = -1 + \eta_d$, and $\eta_u = \eta_u(x,z,t)$ and $\eta_d = \eta_d(x,z,t)$ represent the amount of deformation at the corresponding walls, respectively. The computational coordinate system ξ_i and τ is defined so as to

$$t = \tau, \quad x_1 = \xi_1, \quad x_2 = \xi_2 \left(1 + \eta\right) \eta_0 \quad x_3 = \xi_3 \quad (3)$$

in which $\eta = \left(\eta_u - \eta_d\right)/2$, and $\eta_0 = \left(\eta_u + \eta_d\right)/2$. In the computational space, the upper and lower walls are located at $\xi_2 = 1$ and $\xi_2 = -1$, and the no-slip conditions at the walls can be written as

$$\xi_2 = -1: \quad u = 0, \quad v = \partial \eta_d / \partial t, \quad w = 0 \quad (4)$$

$$\xi_2 = 1: \quad u = 0, \quad v = \partial \eta_u / \partial t, \quad w = 0 \quad (5)$$

By the above coordinate transform, the temporal and spatial derivatives can be represented by

$$\frac{\partial}{\partial t} = \frac{\partial}{\partial \tau} + \varphi_t \frac{\partial}{\partial \xi_2} \quad (6)$$

$$\frac{\partial}{\partial x_i} = \frac{\partial}{\partial \xi_i} + \phi_i \frac{\partial}{\xi_2} \quad (7)$$

in which $\phi_i = \varphi_i - \delta_{i2}$, and

$$\varphi_t = \frac{\partial \xi_2}{\partial t} = -\frac{1}{1+\eta}\left(\xi_2 \frac{\partial \eta}{\partial \tau} + \frac{\partial \eta_0}{\partial \tau}\right) \quad (8)$$

$$\varphi_i = \frac{\partial \xi_2}{\partial x_i} = \begin{cases} -\dfrac{1}{1+\eta}\left(\xi_2 \dfrac{\partial \eta}{\partial \xi_i} + \dfrac{\partial \eta_0}{\partial \xi_i}\right), & i = 1, 3 \\ \dfrac{1}{1+\eta}, & i = 2 \end{cases} \quad (9)$$

The flow quantities in computational space are represented by the expansions of Fourier series and Chebyshev polynomials. Hence for spatial discretization of the governing equations, Fourier-Galerkin method is used in streamwise and spanwise directions, and Chebyshev-Tau method is adopted in wall-normal direction. The extra terms due to coordinate transform are iterated by a modified Newtonian iteration method. The third order time splitting method is employed for time advancement. For more details see Xu (1996).

RESULTS

In present study, a cosine-shaped dimple is imposed at the centre of the lower wall with $D^* = 2$ and $\varepsilon = 0.2$. The dimple profile can be described by

$$\eta_d\left(x, z, t\right) = \begin{cases} -\dfrac{H}{2}\left(1 + \cos\dfrac{2\pi r}{D}\right)\mathcal{T}\left(t\right), & r < D/2 \\ 0, & r \geq D/2 \end{cases} \quad (10)$$

where $r = \sqrt{\left(x - x_0\right)^2 + \left(z - z_0\right)^2}$, $\left(x_0, z_0\right)$ is the centre of the dimple at the plane of channel floor, and $\mathcal{T}\left(t\right)$ is the function describing the temporal variation of the dimple. For, static dimple $\mathcal{T}\left(t\right) = 1$, and for oscillating dimple, $\mathcal{T}\left(t\right) = \left[1 + \sin\left(2\pi t / T\right)\right]/2$. The size of the computational domain for static and oscillating dimple is $2\pi \times 2 \times 2\pi$ and $4\pi \times 2 \times 2\pi$, respectively, in accordance with $64 \times 65 \times 64$ grids. The computations are starting from the laminar plane Poiseuille flow and the flow rates are kept constants during the computation by adjusting the driving pressure gradient every time step according to the friction and pressure drag.

Static Dimple

The flow structures over static dimples are first studied at three different Reynolds numbers, $Re = 500$, 1000 and 1900. As an example, the velocity vectors at (y, z)-plane at different streamwise locations are shown in Fig. 1. The plane at $x = 0$ refers to the plane passing the dimple centre, and positive and negative x values refers to the downstream and upstream locations respectively.

For $Re = 500$, on the plane just in front of the dimple at $x = -1.05$, the fluid flows towards the origin; at $x = -0.79$, the fluid flows into the dimple; at $x = -0.52$, the outside fluid continues the motion into the dimple, but the fluid inside the dimple starts to move upward from the bottom, and form an asymptotic stream surface at about the half depth of the dimple; further downstream, at $x = -0.26$, the upward flow from the dimple bottom becomes even stronger, and the stream surface rises up to about the top of the dimple. At $x = 0$ on the plane passing through the dimple centre, the upward motion from dimple bottom is weaken, because part of the inrush fluid flow out of the dimple along the side walls. Further downstream, at $x = 0.26$, the outside fluid rushes into the dimple at the central part until the dimple bottom, and the outward flow from the dimple along the side wall becomes even stronger. At $x = 0.52$, the inrush motion becomes weaker, and the outward flow along the side wall is more stronger. Near the rear edge of the dimple, the fluid moves purely upward from the dimple bottom as are shown by the vectors on the planes at $x = 0.79$ and $x = 1.05$.

For $Re = 1000$, the whole scenario is similar to that at $Re = 500$, except that on the central plane, a pair of counter-rotating streawise vortices are formed near the side edges for $Re = 1000$. The main difference in flow structures at $Re = 1900$, from those at the other two low Reynolds numbers is the occurrence of the four counter-rotating streamwise vortices in the main flow. A relatively smaller pair of counter-rotating streamwise vortices is located just above the dimple with other two larger vortices on either side. The fluid flow in the dimple is similar to that at $Re = 1000$.

Oscillating Dimple

The oscillating dimple is studied at $Re = 500$ and 1900 with two different oscillating frequencies, $f = 0.5$ and 2.

Fig. 2 shows a sequence of instantaneous three-dimensional iso-surface of $Q = 0.1$ covering one period for $Re = 500$ and $f = 0.5$, in which Q is the second invariant of velocity gradient tensor and is used to identify visualize vortical structures. The periodic shedding of horse-shoe vortices can be easily observed. Under such condition, the horse-shoe vortices only are shed with the same period as the dimple excitation signal. The time series of the instantaneous streamwise velocity component just behind the dimple ($\Delta x = 0.05D$, $\Delta y = 0.056$) are

recorded and shown in Fig. 3 (a). Fourier analysis is also performed on the signal to find the characteristic frequency, as is shown in Fig. 3 (b). From the analysis, it can be deduced that the dominant frequency is the same as the dimple oscillating frequency. With such low Reynolds number and low frequency, the flow remains totally laminar and the information of the flow field follow rigorously the dimple movement.

For $Re = 500$ and $f = 2$, the periodical shedding of vortical structures by oscillating dimples can also be found, but the vortices are more streamwise elongated rather than the horse-shoe like as is shown for example in Fig. 4 (a) the iso-surface of $Q = 0.5$ at a selected phases in one oscillating period. The time evolution of the instantaneous velocity at the point just behind the dimple is shown on Fig. 4 (b), and its Fourier analysis is shown on Fig. 4 (c). Although the flow velocity remains laminar and the dominant frequency is still the oscillating frequency of the dimple at such a low Reynolds number, some fluctuations are introduced by the lower frequency.

Fig. 5 shows the results for the case of $Re = 1900$ and $f = 0.5$. At such a Reynolds number, the flow becomes turbulent due to the disturbance generated by the oscillating dimple. Near the dimple the flow can be strongly affected by the movement but effects of the dimple can be ignored when the distance is increased, as is shown by the iso-surface of $Q = 6$ in Fig. 5 (a). The Fourier analysis shows that no dominant frequency can be identified (see Fig. 5 (c)) in this case. This phenomenon might attribute to the low frequency of dimple oscillation compared with the time scale of the turbulent flow. In one oscillating period the turbulence can be well adjusted and show no relevance with the motion of the dimple. This hypothesis will be further checked.

The results for the increased frequency $f = 2$ at $Re = 1900$ are shown in Fig. 6. In this case, although the flow is turbulent, the vortices shedding from the dimple centre can be observed (Fig. 6 (a)). The velocity just behind the dimple shows a very good periodic behaviour. The spectral analysis of the velocity shows two dominant frequencies of 0.5 and 2 respectively (see Fig. 6 (c)). This new feature raises a lot of questions on the relationship between Reynolds number and the oscillation frequency, more numerical experiments are being carried out to explore this phenomenon.

CONCLUSION

The Reynolds number effects on flow structures over static and oscillating dimples in channel flow at Re=500, 1000 and 1900 have been studied by direct numerical simulation. For static dimple, the velocity vectors on spanwise-normal planes at different streamwise locations show that the fluid flows into the dimple near the leading edge and there are fluids flowing outward before the dimple centre, which is in agreement with the experimental observations by Ligrani (2001). With the increase of the Reynolds number, streamwise vortices can be generated inside the dimple and in the main flow. For oscillating dimple, two frequencies are considered, i.e. f=0.5 and 2. At

Re=500, periodic vortex shedding by the moving dimple can be observed at both frequencies. The flow reacts to the motion of the dimple at the same frequency as the dimple oscillating frequency. At Re=1900, the flow is triggered to turbulent by the dimple in both cases. At low frequency, f=0.5, no obvious interaction between dimple and outside turbulence can be observed. Whereas, increase the frequency to f=2, the influence of dimple motion to outside flow is apparent. Besides the frequency that is the same as the dimple oscillating frequency, f=0.5 can also be observed to play a non-negligible role in the Fourier analysis of the velocity signals. Further analysis to give a possible explanation for this phenomenon is still under going.

REFERENCES

Ligrani, P. M., Harrison, J. L., Mahmmod, G. I., and Hill, M. L., 2001, "Flow Structure due to Dimple Depressions on a Channel Surface ", *Physics of Fluids*, Vol. 13, pp. 3442-3451.

McKeon, B. J., Lambert, S., Sherwin S. J., and Morrison, J. F., 2004, "Active Dimples for Flow Control," *Proceedings, 10th European Turbulence Conference*, H. I. Andersson & P.-A. Krogstad, ed., CIMNE Publication, Barcelona, Spain, pp. 581-584.

Shchukin, A. B., Kozlov, A. B., Chudnovskii, Y. P., and Agachev, R. S., 1998, "Intensification of Heat Exchange by Spherical Depressions. A Survey", *Appl. Energy,* Vol. 36, pp. 45.

Won, S. Y., Zhang, Q., and Ligrani, P. M., 2005, "Comparison of Flow Structure above Dimpled Surfaces with Different Dimple Depths in a Channel ", *Physics of Fluids*, Vol. 17, 045105.

Xu, C., Zhang, Z., Nieuwstadt F. T. M., and Toonder den J. M. J., 1996, "Origin of high kurtosis levels in the viscous sublayer. Direct numerical simulation and experiment ", *Physics of Fluids*, Vol. 8, pp. 1938-1944.

Re=500   Re=1000   Re=1900
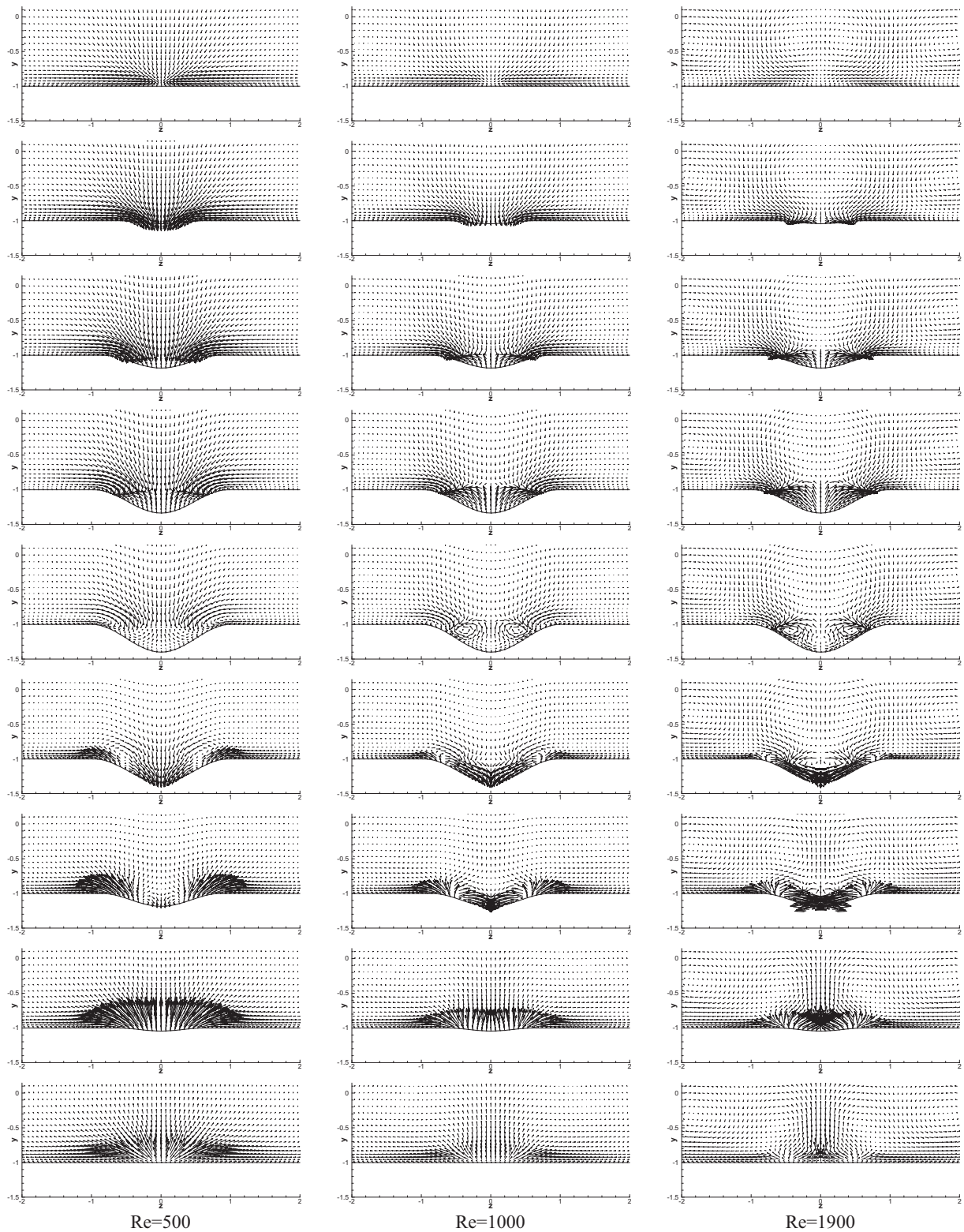
Fig. 1 Velocity vectors on (y,z)-plane at different streamwise locations.
From top to bottom: x=-1.05, -0.79, -0.52, -0.26, 0, 0.26, 0.52, 0.79, 1.05.

638

Sixth International Symposium on Turbulence and Shear Flow Phenomena
Seoul, Korea, 22-24 June 2009
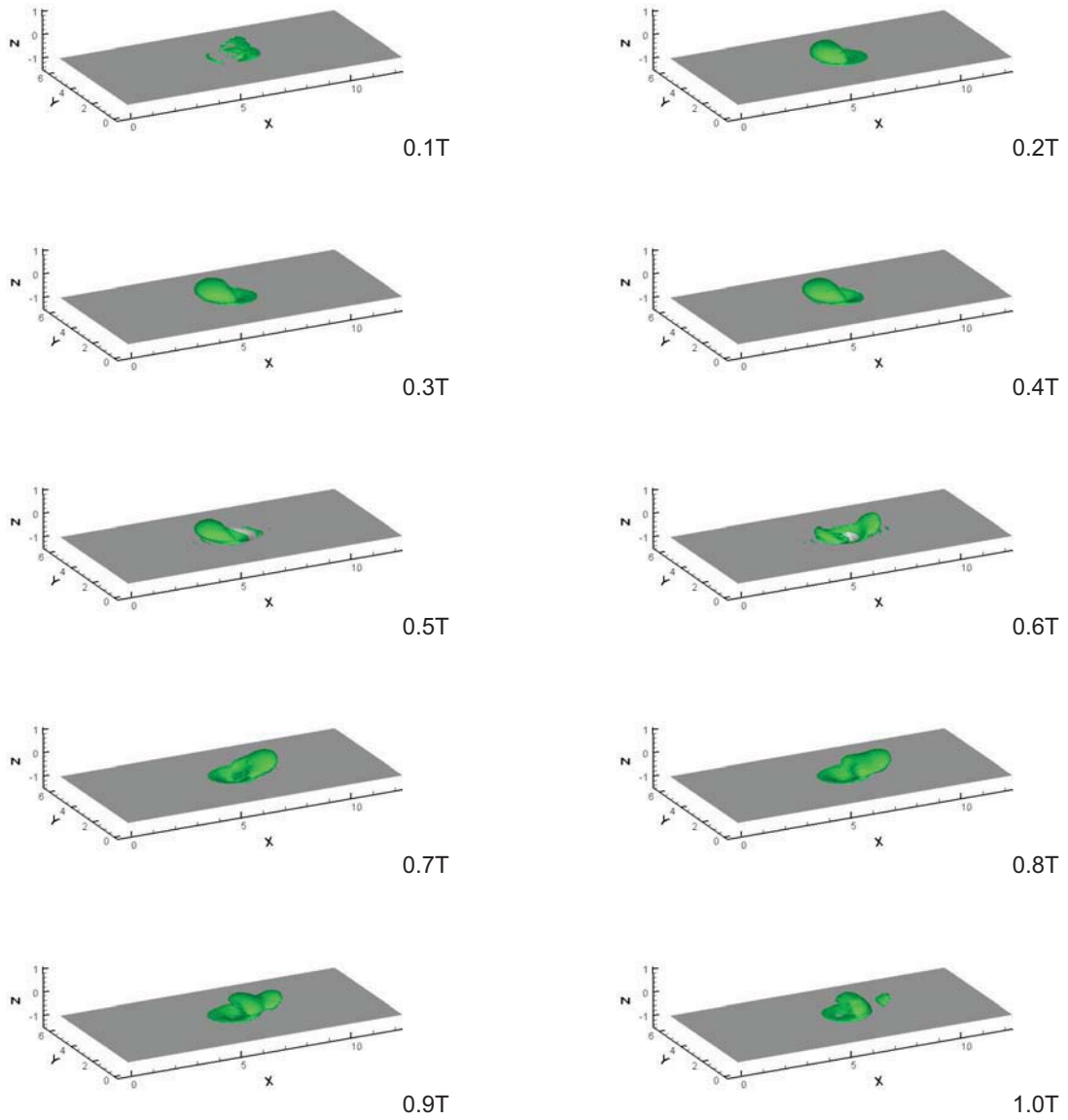
Fig. 2 Iso-surface of Q=0.1 at different time in an oscillating period (Re=500, f=0.5).

(a)   (b)
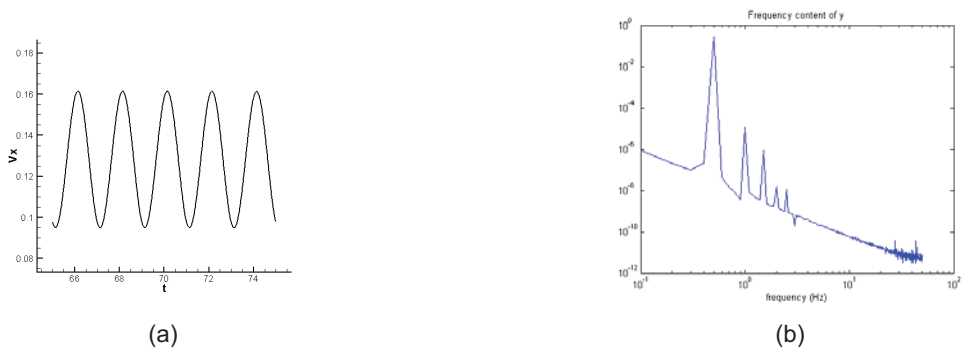
Fig. 3: (a) Time series and (b) Fourier analysis of velocity at a point just behind the dimple (Re=500, f=0.5).

(a)   (b)   (c)
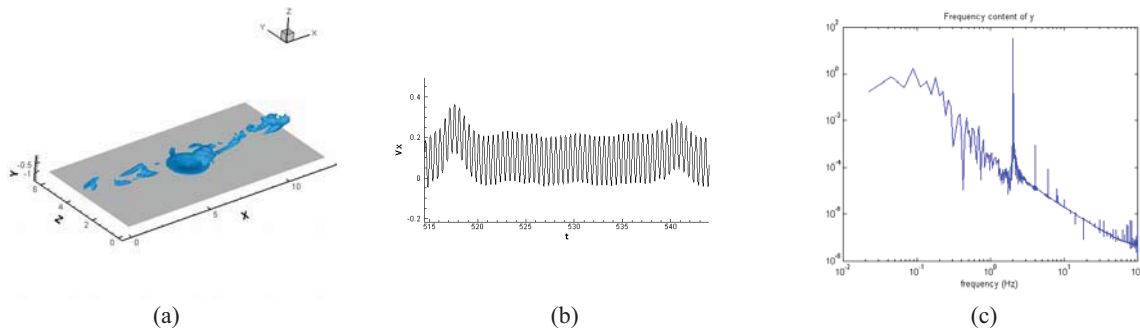
Fig. 4: (a) Iso-surface of Q=0.5, (b) time series and (c) Fourier analysis of velocity at a point just behind the dimple (Re=500, f=2).

(a)   (b)   (c)
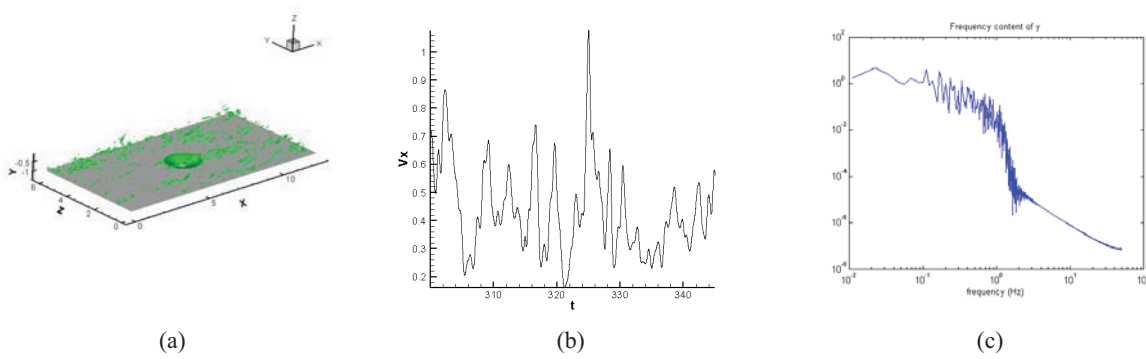
Fig. 5: (a) Iso-surface of Q=6, (b) time series and (c) Fourier analysis of velocity at a point just behind the dimple (Re=1900, f=0.5).

(a)   (b)   (c)

Fig. 6: (a) Iso-surface of Q=6, (b) time series and (c) Fourier analysis of velocity at a point just behind the dimple (Re=1900, f=2).